# Linear Free Energy Relationships in Dinuclear Compounds. 2.[†] Inductive Redox Tuning via Remote Substituents in Quadruply Bonded Dimolybdenum Compounds

**Chun Lin,[‡] John D. Protasiewicz,[§] Eugene T. Smith,[‡] and Tong Ren*,[‡]**

Departments of Chemistry, Florida Institute of Technology, Melbourne, Florida 32901, and Case Western Reserve University, Cleveland, Ohio 44106

*Received May 16, 1996*[⊗]

Syntheses and characterizations are reported for dimolybdenum(II) compounds supported by the diarylformamidinate ($ArNC(H)NAr^-$) ligand, where Ar is $XC_6H_4^-$, with X as *p*−OMe (**1**), H (**2**), *m*-OMe (**3**), *p*-Cl (**4**), *m*-Cl (**5**), *m*-$CF_3$ (**6**), *p*-COMe (**7**), *p*-$CF_3$ (**8**), or Ar is 3,4-$Cl_2C_6H_3^-$ (**9**) or 3,5-$Cl_2C_6H_3^-$ (**10**). The (quasi)reversible oxidation potentials measured for the $Mo_2^{5+}/Mo_2^{4+}$ couple were found to correlate with the Hammett constant ($\sigma_X$) of the aryl substituents according to the following equation: $\Delta E_{1/2} = E_{1/2}(X) - E_{1/2}(H) = 87(8\sigma_X)$ mV. Molecular structure determinations of compounds **1**, **2**, **5**, and **10** revealed an invariant core geometry around the $Mo_2$ center, with statistically identical Mo−Mo quadruple bond lengths of 2.0964(5), 2.0949[8], 2.0958(6), and 2.0965(5) Å, respectively. Magnetic anisotropies for compounds **1**−**10** estimated on the basis of $^1$H NMR data were similar and unrelated to $\sigma_X$. Similarity in UV−vis spectra was also found within the series, which, in conjunction with the features of both molecular structures and $^1$H NMR spectra, was interpreted as the existence of a constant upper valence structure across the series. Results of Fenske−Hall calculations performed for several model compounds paralleled the experimental observations.

## Introduction

Since the seminal discovery of the Re−Re quadruple bond in $Re_2Cl_8^{2-}$,[1] the chemistry of dinuclear compounds containing metal−metal bond has evolved into an important field of inorganic chemistry.[2] Both the nature of metal−metal interactions and their dependence on the coordinating ligands have been elaborated through an extensive study of their syntheses and structural characterization and their spectroscopic, electronic, and magnetic properties over the past three decades. Meanwhile, efforts focusing on technologically important applications of dinuclear compounds have led to many promising research areas, such as inorganic liquid crystals,[3] antitumor agents,[4] materials based on the extended structures[5] and homogeneous[6,7] and photolytic catalysis.[8] There is no doubt that the electronic structure of the dinuclear core plays a key role in these applications and the ability of fine-tuning the electronic structure of the dinuclear core may lead to even greater success for the development of new compounds involved in the above-mentioned applications.

Fine-tuning of the electronic structure is a familiar theme in the coordination chemistry of mononuclear compounds, especially in the design and optimization of homogeneous catalysts[9] and novel materials.[10] Varying the substituents away from the first coordination sphere (remote substituents) is particularly enticing since the energy levels of frontier orbitals may be significantly altered with a minimum change in both the coordination geometry and the *distribution* of metal-based valence orbitals. Furthermore, the degree of tuning can be quantified by correlating the redox potentials of the compounds with the Hammett constant ($\sigma$) of the substituents,[11] which should enable further fine-tuning by exploiting the well-established linear free energy relationship (LFER) in organic chemistry.[12] Substituent tuning in metalloporphyrins has been extensively studied[13] and proven to be critical in developing degradation-resistant metalloporphyrins as the *cyt* $P_{450}$ mimics in hydrocarbon oxygenation.[14] Controlling the electronic richness of square planar Pd organometallic moieties through remote substituents has attracted intense interest recently,[15,16] and the ramification of such control on kinetics is exemplified through

[†] For part 1, see ref 23.
[‡] Florida Institute of Technology.
[§] Case Western Reserve University.
[⊗] Abstract published in *Advance ACS Abstracts,* October 1, 1996.

(1) (a) Cotton, F. A. *Inorg. Chem.* **1965**, *4*, 334. (b) Cotton, F. A.; Harris, C. B. *Inorg. Chem.* **1965**, *4*, 330.
(2) Cotton, F. A.; Walton, R. A. *Multiple Bonds between Metal Atoms*; Oxford University Press: Oxford, 1993.
(3) (a) Giroud-Godquin, A.-M.; Maitlis, P. M. *Angew. Chem., Int. Ed. Engl.* **1991**, *30*, 375. (b) Baxter, D. V.; Cayton, R. H.; Chisholm, M. H.; Huffman, J. C.; Putilina, E. F.; Tagg, S. L.; Wesemann, J. L.; Zwanziger, J. W.; Darrington, F. D. *J. Am. Chem. Soc.* **1994**, *116*, 4551. (c) Bonnet, L.; Cukiernik, F. D.; Maldivi, P.; Giroud-Godquin, A.-M.; Marchon, J.-C.; Ibn-Elhaj, M.; Guillon, D.; Skoulios, A. *Chem. Mater.* **1994**, *6*, 31.
(4) Hall, L. M.; Speer, R. J.; Ridgway, H. J. *J. Clin. Hematol. Oncol.* **1980**, *10*, 25.
(5) (a) Cotton, F. A.; Kim, Y. *J. Am. Chem. Soc.* **1993**, *115*, 8511. (b) Cotton, F. A.; Kim, Y.; Ren, T. *Inorg. Chem.* **1992**, *31*, 2723. (c) Cayton, R. H.; Chisholm, M. H.; Huffman, J. C.; Lobkovsky, E. B. *J. Am. Chem. Soc.* **1991**, *113*, 8709. (d) Mashima, K.; Nakano, H.; Nakamura, A. *J. Am. Chem. Soc.* **1993**, *115*, 11632. (e) Handa, M.; Mikuriya, M.; Kotera, T.; Yamada, K.; Nakao, T.; Matsumoto, H.; Kasuga, K. *Bull. Chem. Soc. Jpn.* **1995**, *68*, 2567.
(6) (a) Doyle, M. P. *Aldrichimica Acta* **1996**, *29*, 3. (b) Doyle, M. P. In *Catalytic Asymmetric Synthesis*; Ojima, I., Ed.; VCH: New York, 1993; and earlier references therein.
(7) Padwa, A.; Austin, D. J. *Angew. Chem., Int. Ed. Engl.* **1994**, *33*, 1797 and earlier references therein.
(8) Nocera, D. G. *Acc. Chem. Res.* **1995**, *28*, 209.
(9) (a) Parshall, G. W.; Ittel, S. D. *Homogeneous Catalysis*; Wiley-Interscience: New York, 1992. (b) Collman, J. P.; Hegedus, L. S.; Norton, J. R.; Finke, R. G. *Principles and Applications of Organotransition Metal Chemistry*; University Science Books: Mill Valley, CA, 1987. (c) Hegedus, L. S. *Transition Metals in the Synthesis of Complex Organic Molecules*; University Science Books: Mill Valley, CA, 1994.
(10) *Inorganic Materials*; Bruce, D. W.; O'Hare, D., Eds.; Wiley: Chichester, 1992.
(11) Zuman, P. *The Elucidation of Organic Electrode Processes*; Academic Press: New York, 1969.
(12) (a) Hammett, L. P. *Physical Organic Chemistry*; McGraw-Hill: New York, 1970. (b) Shorter, J. *Correlation Analysis in Organic Chemistry*; Clarendon Press: Oxford, 1973.
(13) Kadish, K. M. *Prog. Inorg. Chem.* **1986**, *34*, 435 and earlier references therein.

S0020-1669(96)00555-1 CCC: $12.00 

the study of $\beta$-alkyl migratory insertion reactions.[15] Studies of metallodiimine compounds, such as the families of $Ru(bpy)_3^{2+}$ and Pt(diimine)(dithiolate), also demonstrate that a substituent effect can be critical in optimizing the photophysical properties of the well-known MLCT excited state.[17]

Given the abundance of substituent tuning in mononuclear coordination chemistry, it is surprising that there are only few existing examples for the metal−metal bonded dinuclear compounds.[18] Yet the importance of such tuning in dinuclear compounds has been demonstrated with the $Rh_2(O_2CR)_4$-catalyzed intramolecular carbene insertion of 2,3,4-trimethyl-3-pentyl diazoacetoacetate,[7,18c] where both the regio- and chemoselectivities were significantly altered through a variation in the electron-withdrawing ability of R. To our knowledge, there has been no systematic report of substituent tuning for the quadruply bonded species to date. The feasibility, however, is evident from the earlier work for $Mo_2Cl_4(PR_3)_4$,[19] where both the $\delta-\delta^*$ transition energy and the $E_{1/2}(Mo_2^{5+}/Mo_2^{4+})$ linearly correlate with the $\pi$ acidity of $PR_3$. As part of our effort to explore both the general reactivity and the catalytic properties of metal−metal bonded dinuclear compounds, we have initiated extensive studies of the remote substituent effect in dinuclear paddle wheel compounds. The bidentate ligand diarylformamidinate is an excellent candidate for such study, since the phenyl-substituted derivatives can be readily prepared,[20] and its capability to support dinuclear compounds is well documented.[2,21,22] Preliminary results obtained for a series of quadruply bonded dimolybdenum compounds, tetrakis($\mu$−*N*,*N*′-diarylformamidinato)dimolybdenum(II), were communicated earlier,[23] and a full account of the molecular and electronic structures, spectroscopies, redox properties, and their dependence on the remote substituents is presented here.

## Experimental Section

**General Considerations.** All the syntheses were performed under a dry argon atmosphere using standard Schlenk-line techniques unless otherwise specified. Triethyl orthoformate, *p*-anisidine, *m*-anisidine, *p*-toluidine, aniline, *p*-chloroaniline, *m*-chloroaniline, 3-(trifluoromethyl)aniline, 4′-aminoacetophenone, and 3,5-dichloroaniline were purchased from Aldrich, 4-(trifluoromethyl)aniline, and 3,4-dichloroaniline from ACROS, and molybdenum hexacarbonyl from Strem. $^1$H and $^{13}$C NMR spectra were recorded on a Bruker AMX-360 NMR spectrometer, with chemical shifts ($\delta$) referenced to the residual $CHCl_3$ and the solvent $CDCl_3$, respectively. IR spectra were recorded on a Nicolet system 550 (Magna series) FTIR spectrometer using KBr disks. UV−vis spectral data were obtained in degassed $CH_2Cl_2$, using a Hewlett Packard 8452A diode array UV−vis spectrophotometer. Cyclic voltammograms were recorded on a BAS CV-50W voltammetric analyzer with Pt working and auxiliary electrodes and a Ag/AgCl reference electrode in 0.1 M $(n\text{-Bu})_4NBF_4$ $CH_2Cl_2$ solution ($N_2$ degassed). In all the measurements, the potential of ferrocenium/ferrocene couple occurred at 625 mV under the specified experimental conditions.

**Preparation of Ligands.** All the ligands were obtained according to an established procedure.[20] In a typical reaction, 12.32 g (0.10 mol) of *p*-anisidine and 16.6 mL (0.05 mol) of triethyl orthoformate were combined in a round-bottom flask equipped with a distillation tube and heated at 140 °C in air until the distillation of ethanol ceased. The remaining solid was recrystallized from hot toluene, washed with hexane, and dried under a dynamic vacuum to yield 11.29 g of white needles ($(p\text{-OMeC}_6H_4)NC(H)N(H)(p\text{−OMeC}_6H_4)$, 92%). Spectroscopic data (NMR and IR) for all the ligands are listed as part of the supporting information (Table S1).

**Preparation of $Mo_2(ArNC(H)NAr)_4$.** Ar is $XC_6H_4^-$, with X as *p*-OMe (**1**), H (**2**), *m*-OMe (**3**), *p*-Cl (**4**), *m*-Cl (**5**), *m*-$CF_3$ (**6**), *p*-COMe (**7**), *p*-$CF_3$ (**8**), Ar is 3,4-$Cl_2C_6H_3^-$ (**9**) or 3,5-$Cl_2C_6H_3^-$ (**10**). Except **7**, all the compounds were obtained as yellow polycrystalline materials through refluxing $Mo(CO)_6$ with 3 equiv of the corresponding ligands in degassed (two freeze−pump−thaw cycles) *o*-dichlorobenzene. Yields (based on $Mo(CO)_6$) varied from 70% to 95%. Refluxing the formamidine bearing the *p*-acetyl group with $Mo(CO)_6$ led to intractable brown products. Compound **7** was obtained in 65% yield by treating $Mo_2(OAc)_4$ with the lithiated formamidine (4 equiv) in degassed THF. Compounds **1** and **4** were submitted for elemental analysis (performed by Atlantic Microlab, Norcross, GA) with the following results: **1**, calcd (found), C, 59.41 (59.48), N, 9.24 (9.22), H, 4.98 (4.98); **4**, C, 50.03 (50.30), N, 8.98 (8.84), H, 2.91 (3.04). Single crystals of X-ray quality were grown by slow diffusion of hexane into a $CH_2Cl_2$ solution for compounds **1**, **2**, **5**, and **10**. The analog with X as *p*-Me (**11**), a known compound, was prepared and purified according to the literature.[24] UV−vis spectral data are given in Table 3 for all the compounds but **9**, for which the data are inaccessible due to very low solubility of the compound in common organic solvents. $^1$H and $^{13}$C NMR and IR spectroscopic data are supplied as part of the supporting information (Table S2).

**X-ray Crystallography for Compounds 1, 2, 5, and 10.** All the diffraction data sets were collected with a Siemens P4 instrument (Mo K$\alpha$ radiation ($\lambda = 0.710\ 73$ Å). Typically, a brick-shaped yellow crystal was glued onto the tip of a glass fiber. The crystal was judged to be acceptable on the basis of omega scans and rotation photography. A random search located reflections to generate the reduced primitive cell, cell lengths being corroborated by axial photography. Additional reflections with $2\theta$ values near 25° were appended to the reflection array and yielded the refined cell constants. Data were collected as presented in Table 1 and were corrected for absorption (empirical $\psi$ scan).

Computations were performed using SHELXTL PLUS, PC Version 5.1$\beta$ (Siemens Analytical), and data were refined against $F^2$ ($wR_2 = [\sum[w(F_o^2 - F_c^2)^2]/\sum[w(F_o^2)^2]^{1/2}$). All of the non-hydrogen atoms were located with direct methods and refined anisotropically. Hydrogen atoms were located and refined with $B_{eq} = 1.2 \times$ the value of attached carbon atoms, except for the methoxyl protons of **1**, which were disordered and idealized atoms that were generated and refined with $B_{eq} = 0.08$. For compounds **1**, **5**, and **10**, there is only one-half of the molecule in the asymmetric unit, which is related to the other half via the crystallographic inversion center situated at the centroid of the Mo−Mo′ vector. There are two half-molecules in the asymmetric units of **2**, and each is similarly related to the other half through inversion. The final least-squares refinement converged at the *R*-factors reported in Table 1, along with other procedure parameters. Atomic coordinates and isotropic displacements are provided as supporting information (Tables S3−S22). Table 2 lists selected bond lengths and angles for compounds **1**, **2**, **5**, and **10**. Since the geometrical parameters for two independent molecules of **2** are essentially the same, only those for one of them are included in Table 2.

**Computational Procedure.** Fenske−Hall molecular orbital calcula-

(14) (a) Ostovic, D.; Bruice, T. C. *Acc. Chem. Res.* **1992**, *25*, 314. (b) Grinstadff, M. W.; Hill, M. G.; Birnbaum, E. R.; Schaefer, W. P.; Labinger, J. A.; Gray, H. B. *Inorg. Chem.* **1995**, *34*, 4896.
(15) Rix, F. C.; Brookhart, M.; White, P. S. *J. Am. Chem. Soc.* **1996**, *118*, 2436.
(16) (a) Baranano, D.; Hartwig, J. F. *J. Am. Chem. Soc.* **1995**, *117*, 2937. (b) Kapteijn, G. M.; Spee, M. P. R.; Grove, D. M.; Kooijman, H.; Spek, A. L.; van Koten, G. *Organometallics* **1996**, *15*, 1405.
(17) (a) Nazeeruddin, M. K.; Zakeeruddin, S. M.; Kalyanasundaram, K. *J. Phys. Chem.* **1993**, *97*, 9607. (b) Cummings, S. D.; Eisenberg, R. *J. Am. Chem. Soc.* **1996**, *118*, 1949.
(18) (a) Das, K.; Kadish, K. M.; Bear, J. L. *Inorg. Chem.* **1978**, *17*, 930. (b) Bottomley, L. A.; Hallberg, T. A. *Inorg. Chem.* **1984**, *23*, 1584. (c) Pirrung, M. C.; Morehead, A. T. *J. Am. Chem. Soc.* **1994**, *116*, 8991.
(19) (a) Cotton, F. A.; Daniels, L. M.; Powell, G. L.; Kahaian, A. J.; Smith, T. J.; Vogel, E. F. *Inorg. Chim. Acta* **1988**, *144*, 109. (b) Hanselman, D. S.; Smith, T. J. *Polyhedron* **1988**, *7*, 2679. Both the inductive effect and the steric bulkness (Tolman's cone angle) of R contribute to the $\pi$ acidity of $PR_3$.
(20) Bradley, W.; Wright, I. *J. Chem. Soc.* **1956**, 640.
(21) (a) Barker, J.; Kilner, M. *Coord. Chem. Rev.* **1994**, *133*, 219. (b) Umakoshi, K.; Sasaki, Y. *Adv. Inorg. Chem.* **1993**, *40*, 187.
(22) Cotton, F. A.; Ren, T. *J. Am. Chem. Soc.* **1992**, *114*, 2237.
(23) Lin, C.; Protasiewicz, J. D.; Smith, E. T.; Ren, T. *J. Chem. Soc., Chem. Commun.* **1995**, 2257.
(24) Cotton, F. A.; Feng, X.; Matusz, M. *Inorg. Chem.* **1989**, *28*, 594.

**Table 1.** Crystallographic Data for Compounds **1**, **2**, **5**, and **10**

| | **1** | **2** | **5** | **10** |
|---|---|---|---|---|
| formula | $C_{60}H_{60}N_8O_8Mo_2$ | $C_{52}H_{44}N_8Mo_2$ | $C_{52}H_{36}Cl_8N_8Mo_2$ | $C_{52}H_{28}Cl_{16}N_8Mo_2$ |
| formula weight | 1213.04 | 972.83 | 1248.37 | 1523.90 |
| cryst syst | triclinic | monoclinic | triclinic | triclinic |
| space group | $P\bar{1}$ | $P2_1/n$ | $P\bar{1}$ | $P\bar{1}$ |
| *a*, Å | 10.314(1) | 18.101(1) | 9.962(3) | 9.885(1) |
| *b*, Å | 10.405(1) | 10.404(1) | 11.555(3) | 11.773(1) |
| *c*, Å | 13.996(1) | 24.498(2) | 12.463(3) | 14.463(1) |
| α, deg | 80.65(1) | | 87.80(3) | 97.58(1) |
| *β*, deg | 75.76(1) | 101.99(1) | 75.90(3) | 104.67(1) |
| *γ*, deg | 81.55(1) | | 65.85(2) | 113.53(1) |
| volume, Å$^3$ | 1427.4(3) | 4512.7(7) | 1266.6(5) | 1440.3(2) |
| *Z* | 1 | 4 | 1 | 1 |
| $\rho_{calc}$, g cm$^{-3}$ | 1.411 | 1.432 | 1.637 | 1.757 |
| $\mu$, mm$^{-1}$ | 0.500 | 0.601 | 0.963 | 1.223 |
| $\lambda$, Å | 0.71073 | 0.71073 | 0.71073 | 0.71073 |
| $\theta$ range, deg | 2.00−25.00 | 1.96−24.00 | 1.94−25.00 | 1.96−23.99 |
| *T*, K | 293(2) | 293(2) | 293(2) | 293(2) |
| R1[a] | 0.0395 | 0.0377 | 0.0310 | 0.0279 |
| wR2[b] | 0.1127 | 0.0763 | 0.0903 | 0.0691 |
| goodness of fit on $F^2$[c] | 1.427 | 1.070 | 1.281 | 1.216 |

[a] $R1 = \sum||F_o| - |F_c||/\sum|F_o|$. [b] $wR2 = [\sum[w(F_o^2 - F_c^2)^2]/\sum[w(F_o^2)^2]]^{1/2}$. [c] goodness of fit $= [\sum[w(F_o^2 - F_c^2)^2]/(n - p)]^{1/2}$.

**Table 2.** Selected Geometric Parameters for Molecules **1**, **2**, **5**, and **10**

| **1** | | **2** | | **5** | | **10** | |
|---|---|---|---|---|---|---|---|
| Mo(1)−Mo(1)′ | 2.0964(5) | Mo(1)−Mo(1)′ | 2.0944(8) | Mo(1)−Mo(1)′ | 2.0958(6) | Mo−Mo′ | 2.0965(5) |
| Mo(1)−N(1) | 2.154(3) | Mo(1)−N(5) | 2.161(4) | Mo(1)−N(1) | 2.165(2) | Mo−N(11) | 2.157(2) |
| Mo(1)−N(2)′ | 2.163(3) | Mo(1)−N(6) | 2.152(4) | Mo(1)−N(2)′ | 2.152(2) | Mo−N(21) | 2.163(2) |
| Mo(1)−N(3) | 2.150(3) | Mo(1)−N(7) | 2.167(4) | Mo(1)−N(3) | 2.165(2) | Mo−N(31) | 2.174(2) |
| Mo(1)−N(4) | 2.166(3) | Mo(1)−N(8) | 2.138(4) | Mo(1)−N(4)′ | 2.163(2) | Mo−N(41) | 2.170(2) |
| N(1)−C(1) | 1.327(4) | N(5)−C(4)′ | 1.318(6) | N(1)−C(1) | 1.326(3) | N(11)−C(3)′ | 1.325(4) |
| N(2)−C(1) | 1.328(4) | N(6)−C(3)′ | 1.330(6) | N(2)−C(1) | 1.327(3) | N(21)−C(4)′ | 1.324(4) |
| N(3)−C(2)′ | 1.324(4) | N(7)−C(3) | 1.329(6) | N(3)−C(2) | 1.330(3) | N(31)−C(3) | 1.327(4) |
| N(4)−C(2) | 1.333(4) | N(8)−C(4) | 1.333(6) | N(4)−C(2) | 1.323(3) | N(41)−C(4) | 1.325(4) |
| Mo(1)′−Mo(1)−N(1) | 91.44(7) | Mo(1)′−Mo(1)−N(5) | 91.57(10) | Mo(1)′−Mo(1)−N(1) | 92.82(6) | Mo′−Mo−N(11) | 92.26(6) |
| Mo(1)′−Mo(1)−N(2)′ | 93.99(7) | Mo(1)′−Mo(1)−N(6) | 94.44(10) | Mo(1)′−Mo(1)−N(2)′ | 92.53(6) | Mo′−Mo−N(21) | 92.80(6) |
| Mo(1)′−Mo(1)−N(3) | 92.86(7) | Mo(1)′−Mo(1)−N(7) | 91.28(10) | Mo(1)′−Mo(1)−N(3) | 92.22(6) | Mo′−Mo−N(31) | 93.15(6) |
| Mo(1)′−Mo(1)−N(4) | 92.72(7) | Mo(1)′−Mo(1)−N(8) | 93.88(10) | Mo(1)′−Mo(1)−N(4)′ | 93.27(6) | Mo′−Mo−N(41) | 92.42(6) |
| N(3)−Mo(1)−N(1) | 89.90(10) | N(6)−Mo(1)−N(5) | 91.34(14) | N(1)−Mo(1)−N(4)′ | 89.22(9) | N(11)−Mo−N(21) | 89.93(9) |
| N(3)−Mo(1)−N(2)′ | 88.88(10) | N(5)−Mo(1)−N(7) | 177.12(14) | N(1)−Mo(1)−N(3) | 90.73(9) | N(11)−Mo−N(41) | 89.59(9) |
| N(1)−Mo(1)−N(2)′ | 174.49(9) | N(6)−Mo(1)−N(7) | 88.04(14) | N(2)′−Mo(1)−N(1) | 174.62(7) | N(11)−Mo−N(31) | 174.54(8) |
| N(3)−Mo(1)−N(4) | 174.31(9) | N(8)−Mo(1)−N(5) | 88.78(14) | N(2)′−Mo(1)−N(3) | 89.68(9) | N(21)−Mo−N(31) | 89.12(9) |
| N(1)−Mo(1)−N(4) | 91.09(10) | N(8)−Mo(1)−N(6) | 171.66(14) | N(2)′−Mo(1)−N(4)′ | 89.87(9) | N(21)−Mo−N(41) | 174.77(8) |
| N(2)′−Mo(1)−N(4) | 89.60(10) | N(8)−Mo(1)−N(7) | 91.43(14) | N(4)′−Mo(1)−N(3) | 174.51(7) | N(41)−Mo−N(31) | 90.86(9) |
| C(1)−N(1)−Mo(1) | 118.6(2) | C(4)′−N(5)−Mo(1) | 117.7(3) | C(1)−N(1)−Mo(1) | 116.9(2) | C(3)′−N(11)−Mo | 117.9(2) |
| C(1)−N(2)−Mo(1)′ | 115.8(2) | C(3)′−N(6)−Mo(1) | 115.6(3) | C(1)−N(2)−Mo(1)′ | 117.8(2) | C(4)′−N(21)−Mo | 117.4(2) |
| C(2)′−N(3)−Mo(1) | 117.4(2) | C(3)−N(7)−Mo(1) | 117.8(3) | C(2)−N(3)−Mo(1) | 117.3(2) | C(3)−N(31)−Mo | 116.2(2) |
| C(2)−N(4)−Mo(1) | 116.5(2) | C(4)−N(8)−Mo(1) | 116.4(3) | C(2)−N(4)−Mo(1)′ | 116.6(2) | C(4)−N(41)−Mo | 117.3(2) |
| N(1)−C(1)−N(2) | 120.2(3) | N(7)−C(3)−N(6)′ | 120.7(5) | N(1)−C(1)−N(2) | 120.0(2) | N(11)′−C(3)−N(31) | 120.4(3) |
| N(3)′−C(2)−N(4) | 120.5(3) | N(5)′−C(4)−N(8) | 120.4(4) | N(4)−C(2)−N(3) | 120.5(2) | N(21)′−C(4)−N(41) | 119.9(3) |

tions[25] were carried out with a VAX station 4000 VLC. Basis functions used were generated by the numerical Xα atomic orbital program[26] in conjunction with an Xα-to-Slater basis program.[27]

Calculations were performed for compounds **1**, where −OMe was replaced with −OH due to the limit on the maximum number of basis functions, **4**, **5**, and **10**. Due to the invariance of $Mo_2$ core geometry (see Results and Discussion), the following metric parameters were kept identical in all the model compounds: Mo−Mo, 2.095 Å; Mo−N, 2.17 Å; Mo−Mo−N, 92.4°; and an eclipsed configuration. The dihedral angle between the phenyl ring and the adjacent N−Mo−Mo plane was set to 30° in keeping with the canted orientation of phenyl groups observed in the X-ray structures, and all the model compounds possess a $D_4$ point symmetry. Typical distances for C−C, C−H, C−Cl, and O−H bonds were assumed.[28]

## Results and Discussion

**Synthesis.** The synthetic routes (**A** and **B**) applied in the present study (sketched below) are the same as that reported for the *p*-Me analog,[24] and the yields were excellent. The failure to isolate *p*-acetyl derivative (**7**) via route **A** is due to the thermal instability of the ligand. All of the compounds except **9** are fairly soluble in common polar solvents, which facilitated both the spectroscopic and electrochemical characterizations. Satisfactory elemental analysis was obtained for two of the

$$Mo(CO)_6 + Hform \xrightarrow[\mathbf{A}]{o\text{-}Cl_2C_6H_4} Mo_2(form)_4 \xleftarrow[\mathbf{B}]{THF} Mo_2(OAc)_4 + Li^+form^-$$

(25) Hall, M. B.; Fenske, R. F. *Inorg. Chem.* **1972**, *11*, 768.
(26) Herman, F.; Skillman, S. *Atomic Structure Calculations*; Prentice-Hall: Englewood Cliffs, NJ, 1963.
(27) (a) Bursten, B. E.; Fenske, R. F. *J. Chem. Phys.* **1977**, *67*, 3138. (b) Bursten, B. E.; Jensen, J. R.; Fenske, R. F. *J. Chem. Phys.* **1978**, *68*, 3320.
(28) *International Tables for X-Ray Crystallography*; Kynoch: Birmingham, 1968; Vol. 3.

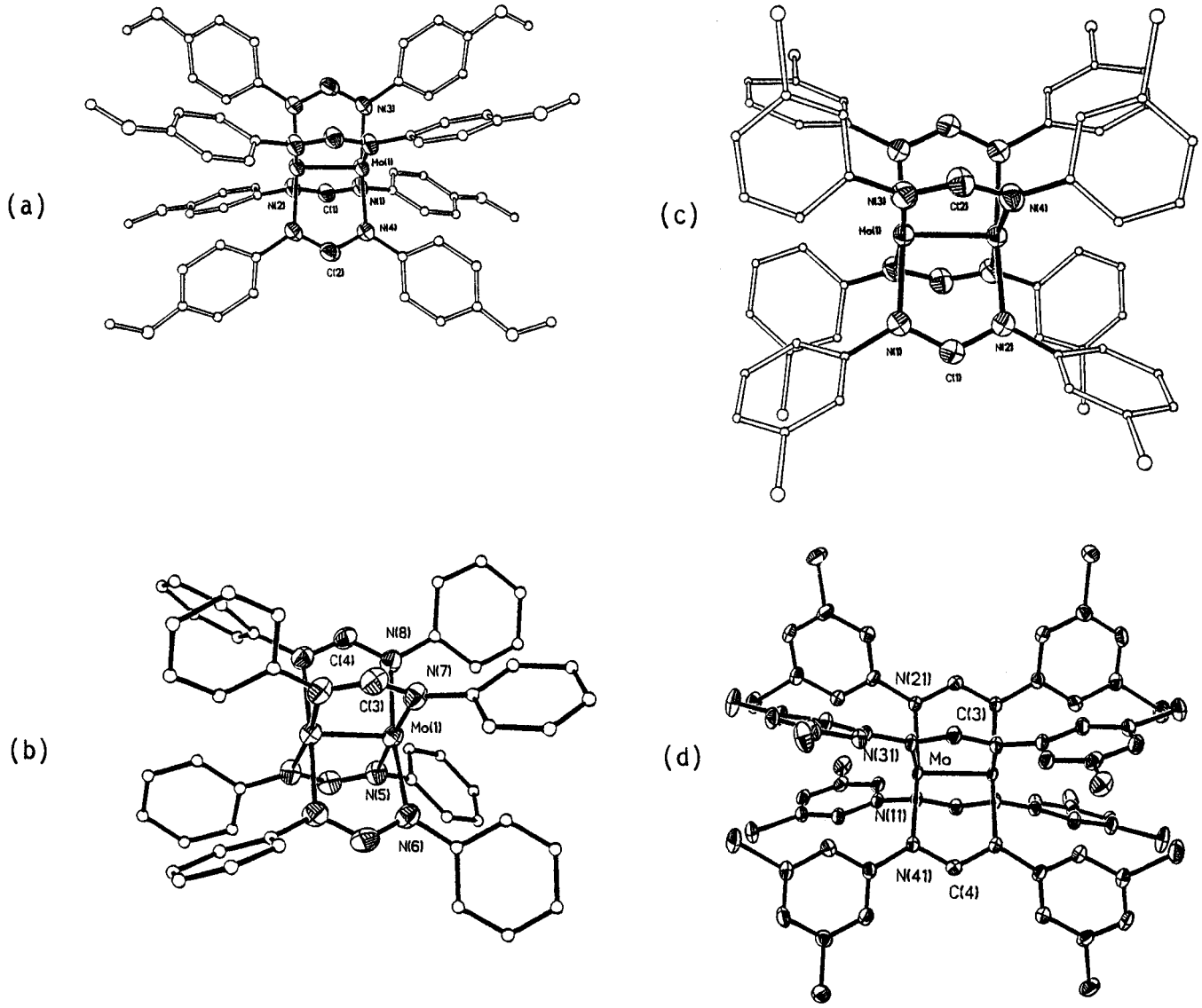


**Figure 1.** Structural diagrams for the molecular structures determined: (a) **1**, (b) **2**, (c) **5**, (d) **10**.

compounds (**1** and **4**), while the purity of the rest of compounds is obvious from their $^1$H NMR spectra.

**Molecular Structures.** In contrast to the *p*-Me analog which crystallizes in tetragonal space group ($P4/n$),[24] all the compounds crystallographically characterized in the present work crystallize in lower symmetries, which reflects the sensitivity of the packing pattern toward the identity and position of phenyl substituents and reflects, perhaps, the choice of crystallization solvents as well.

Structural diagrams of compounds **1**, **2**, **5**, and **10** are shown in Figure 1 parts **a**−**d**. Similar to the *p*-Me analog (**11**), all the compounds adopt the paddle wheel motif. Mo−Mo distances are 2.0964(5), 2.0949[8], 2.0958(6), and 2.0965(5) Å for **1**, **2**, **5**, and **10**, respectively, which are typical for a Mo−Mo quadruple bond and longer than, but statistically identical to, that of **11** (2.085(4) Å).[24] Similarity in the Mo−N bond lengths also exists among **1**, **2**, **5**, **10**, and **11**: the averaged values are 2.158[3], 2.155[4], 2.161[2], 2.166[2], and 2.171[14] Å, respectively. An essentially eclipsed coordination geometry for the $Mo_2$ core was also observed for all the compounds, where the averaged torsional angles N−Mo−Mo′−N′ are 1.1°, 1.4°, 0.4°, and 0.5° for **1**, **2**, **5**, and **10**, respectively. Considering the large variance of $\sigma_X$ among the compounds structurally characterized, it is clear that there is little, if any, substituent effect on the geometry about the dimolybdenum core.

**$^1$H NMR Spectra.** All the compounds in the series display only one set of aromatic chemical shifts in their $^1$H NMR spectra, which implies an effective 8-fold molecular symmetry, either $D_4$ or $C_{4h}$. Although compounds **3**, **4**, and **6**−**9** have not been crystallographically characterized, the observed trend indicates that they are isostructural to **1**, **2**, **5**, and **10**.

It has been demonstrated that the chemical shifts of the protons in the vicinity of the dinuclear core are sensitive to the magnetic anisotropy ($\Delta\chi$) produced by the metal−metal multiple bond and may thus serve as a sensitive probe of the bond multiplicity.[22,29] $\Delta\chi$ for a variety of dinuclear compounds were estimated on the basis of the $\delta$ of methine proton (−NC**H**N−) of the formamidinate group according to the following equation:[30]

$$\Delta\chi = \chi_{\parallel} - \chi_{\perp} = \frac{12\pi r^3 \Delta\delta}{(1 - 3\cos^2\theta)} \qquad (1)$$

where $\Delta\delta = \delta(-\text{NC}\mathbf{H}\text{N}-\text{ in } M_2) - \delta(-\text{NC}\mathbf{H}\text{N}-\text{ in } Ni_2)$ and the $r$ is the estimated distance between the methine proton

(29) (a) Cotton, F. A.; Kitagawa, S. *Polyhedron* **1988**, *7*, 1673. (b) Cotton, F. A.; Kitagawa, S. *Inorg. Chem.* **1987**, *26*, 3463.
(30) Harris, R. K. *Nuclear Magnetic Resonance Spectroscopy*; Pittman: London, 1983.

**Table 3.** Spectroscopic and Electrochemical Data of $Mo_2$(diarylformamidinate)$_4$

| | compound (X) | | | | | | | | | |
|---|---|---|---|---|---|---|---|---|---|---|
| | **1** ($p$−$OCH_3$) | **11** ($p$-$CH_3$[a]) | **2** (−H) | **3** ($m$$OCH_3$) | **4** ($p$-Cl) | **5** ($m$-Cl) | **6** ($m$-$CF_3$) | **7** ($p$-$COCH_3$) | **8** ($p$-$CF_3$) | **10** (3,5-$Cl_2$) |
| $\sigma$ | −0.27 | −0.17 | 0 | 0.12 | 0.23 | 0.37 | 0.43 | 0.50 | 0.54 | 0.74 |
| $E_{1/2}$, mV[b] | 244 | 333 | 418 | 458 | 601 | 683 | 762 | 778 | 795 | |
| ($\Delta E_p$ (mV), $i_{p,c}/i_{p,a}$) | (158, 0.98) | (191, 0.97) | (93, 0.96) | (197, 1.01) | (250, 1.19) | (177, 0.99) | (155, 0.75) | (137, 0.73) | (155, 0.77) | |
| $\Delta\chi$ ($10^{-36}$ $m^3$/molecule) | 4950 | 5060 | 5000 | 5040 | 4900 | 4890 | 4820 | | 4750 | 4730 |
| $\lambda_{max}$ ($\delta$−$\delta$*), nm[c] | 430 (sh) | 438 (sh) | 440 (sh) | 442 (sh) | 438 (sh) | 442 (sh) | 442 (sh) | 436 (sh) | 446 (sh) | 444 (sh) |
| $\lambda_{max}$ (others), nm, ($\epsilon$, $M^{-1}$ $cm^{-1}$)[c] | 274 (sh) | 270 (sh) | 270 (sh) | 280 (sh) | 270 (sh) | 270 (sh) | 272 (52 500) | 308 (sh) | 268 (54 400) | 272 (sh) |
| | 288 (67 900) | 290 (63 200) | 288 (46 700) | 294 (56 000) | 294 (74 300) | 290 (69 600) | 288 (53 500) | 336 (106200) | 296 (70100) | 292 (53800) |
| | 310 (sh) | 316 (sh) | 312 (sh) | 318 (sh) | 320 (sh) | 312 (sh) | 308 (sh) | | 314 (sh) | 320 (sh) |
| | 384 (sh) | 375 (sh) | 370 (sh) | 384 (sh) | 384 (sh) | 384 (sh) | 384 (sh) | | 386 (sh) | 382 (sh) |

[a] Spectroscopic and electrochemical data for this compound were reported in ref 24, but were redetermined here to ensure a consistent experimental condition across the series. Only minor deviation was noticed. [b] Measurement was carried out in $CH_2Cl_2$ with $Bu_4NBF_4$ as the supporting electrolyte, Pt working and auxiliary electrodes, Ag/AgCl reference electrode, [$Mo_2$] ≈ 1 mM, and scan rate 100 mV/s. Under these conditions, the $E_{1/2}$($Fc^+$/$Fc$) was consistently measured at +625 mV. $E_{1/2} = (E_{p,a} + E_{p,c})/2$ and $\Delta E_p = E_{p,a} - E_{p,c}$. [c] UV−vis spectra were recorded in degassed $CH_2Cl_2$.

and the centroid of the M−M vector.[22] As discussed earlier,[22] the change of the chemical shift ($\Delta\delta$) due to the magnetic anisotropy is best referenced to the dinickel analogs ($Ni_2$(form)$_4$), where the magnetic anisotropy vanishes due to the absence of Ni−Ni covalent bonding. Most of the dinickel analogs corresponding to the present dimolybdenum series have been synthesized and characterized,[31] and hence the $\Delta\chi$ for the dimolybdenum center can be estimated according to eq 1 and the values are listed in Table 3. The magnetic anisotropy does vary across the series, but the variance is relatively small and seems unrelated to the Hammett constant of substituents. Thus the accumulation of the bonding electron density along the Mo−Mo vector is essentially a *constant*, reinforcing our belief that the Mo−Mo quadruple bond is not affected by remote substituents.

**Redox Properties.** Early studies established that the *p*-Me analog undergoes a reversible one-electron (1e) oxidation, which led to the isolation of the oxidized monocation. Structural

$$Mo_2(L)_4 \underset{+\,e^-}{\overset{-e^-}{\rightleftharpoons}} [Mo_2(L)_4]^+ \qquad (2)$$

comparison between the neutral parent molecule and the daughter cation led to the unambiguous assignment that the oxidation corresponds to the removal of an electron from the Mo−Mo $\delta$ bonding orbital,[24] and hence the half-wave potential ($E_{1/2}$) determined from a cyclic voltammogram (CV) should provide an accurate assessment of the absolute energy of $\delta$ bonding orbital. Similarly, the first eight compounds (**1**−**8**) in the current series were found to undergo 1e (qausi)reversible oxidation in dichloromethane solution. Typical CV profiles of **1**, **8**, and **10** are shown in Figure 2, while the measured parameters ($E_{1/2}$, $i_{pc}/i_{pa}$) are listed in Table 3. The measured $E_{1/2}$ values range from +244 mV for **1** to +795 mV for **8** and are shifted anodically as $\sigma_X$ increases. Therefore, the energy of $\delta$ bonding orbital decreases significantly upon increasing the electron-withdrawing ability of the substituent.

A linear least-squares fitting of the $E_{1/2} - 8\sigma_X$ plot (coefficient 8 is the number of substituents per compound, see ref 23 for the plot) revealed the following Hammett equation[11] with a correlation coefficient of 0.993:

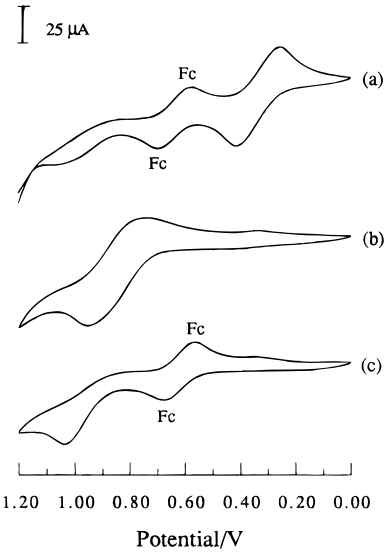


**Figure 2.** Some typical cyclovoltammograms for dimolybdenum compounds: (a) **1**, (b) **7**, (c) **10**. Peaks corresponding to the ferrocene standard are marked with "Fc". Ferrocene standard is not shown in (b) since its peaks severely overlap with those of the sample.

$$\Delta E_{1/2} = E_{1/2}(X) - E_{1/2}(H) = \rho 8\sigma_X,\ \rho = 87.2\ \text{mV} \qquad (3)$$

The reactivity constant $\rho$ is comparable to those determined for the metal-based redox processes in various substituted metalloporphyrins[13] and is larger than that estimated for the oxidation of $Rh_2(O_2CR)_4$ (64 mV).[18] However, $\rho(Mo_2)$ is significantly smaller than the reactivity constant determined for the $Ni_2$(form)$_4$ analogs (114 mV),[31] which contrasts the pattern observed for metalloporphyrins where the redox reactivity constant decreases as the number of d orbital electrons increases.[13] This discrepancy probably originates from the difference in the Ni-based HOMO between the current series and Ni−porphyrine series. On the basis of eq 3, a (quasi)-reversible oxidation around 944 mV would be anticipated for compound **10** ($\sigma = 2\sigma_m(Cl) = 0.74$; assuming that the additivity of Hammett constants is valid, see ref 12), but only an anodic peak was observed at 1029 mV.

Consistent with the measured $E_{1/2}$ values, the resistance toward aerobic oxidation gradually increases with increasing $\sigma$ value across the series. For instance, a solution of **1** in anhydrous $CH_2Cl_2$ turns to brown within minutes when exposed to air, while the solution of **10** displays an identical UV−vis spectrum even after weeks of exposure to air.

(31) Lin, C.; Protasiewicz, J. D.; Ren, T. *Inorg. Chem.* submitted for publication. $\delta$(−NC**H**N−) (ppm, in $CDCl_3$) are 6.15 ($p$-$OCH_3$), 6.17 ($p$-$CH_3$), 6.28 (−H), 6.31 ($m$-$OCH_3$), 6.22 ($p$-Cl), 6.33 ($m$-Cl), 6.45 ($m$-$CF_3$), 6.48 ($p$-$CF_3$), 6.41 (3,5-$Cl_2$).

**Table 4.** Upper Valence Molecular Orbitals for Dimolybdenum Compounds **1**, **4**, **5**, and **10**

| | compound | | | | | | | |
|---|---|---|---|---|---|---|---|---|
| | **1** | | **4** | | **5** | | **10** | |
| assign. | *E* (eV) | characters (%) | *E* (eV) | characters (%) | *E* (eV) | characters (%) | *E* (eV) | characters (%) |
| $\pi^*$(e) | 1.12 | $d_{xz,yz}$ (76) | 0.59 | $d_{xz,yz}$ (57) | −0.03 | $d_{xz,yz}$ (62) | 0.04 | $d_{xz,yz}$ (89) |
| $\sigma^*(a_2)$ | −1.36 | $d_{z^2}$ (41), Mo pz (33), Mo s (10) | −1.87 | $d_{z^2}$ (42), Mo pz (34), Mo s (10) | −2.13 | $d_{z^2}$ (45), Mo pz (37), Mo s (11) | −2.19 | $d_{z^2}$ (45), Mo pz (36), Mo s (10) |
| $\delta^*$ ($b_1$, LUMO) | −2.20 | $d_{xy}$ (76), $Np_{x,y}$ (14) | −2.82 | $d_{xy}$ (76), $Np_{x,y}$ (13) | −3.30 | $d_{xy}$ (77), $Np_{x,y}$ (12) | −3.38 | $d_{xy}$ (78), $Np_{x,y}$ (12) |
| $\delta$ ($b_2$, HOMO) | −7.12 | $d_{xy}$ (86), $C_{methine}p_{x,y}$ (14) | −7.66 | $d_{xy}$ (86), $C_{methine}p_{x,y}$ (14) | −7.99 | $d_{xy}$ (86), $C_{methine}p_{x,y}$ (13) | −8.05 | $d_{xy}$ (87), $C_{methine}p_{x,y}$ (13) |
| ($a_1$) | −8.54 | $Np_{x,y}$ (48) | −9.20 | $Np_{x,y}$ (45) | −10.43 | $Np_{x,y}$ (59) | −10.63 | $Np_{x,y}$ (58) |
| (e) | −8.93 | $Np_{x,y}$ (42) | −9.55 | $Np_{x,y}$ (38) | −10.78 | $Np_{x,y}$ (47) | −10.96 | $Np_{x,y}$ (41) |
| $\pi$(e) | −10.12 | $d_{xz,yz}$ (93) | −10.67 | $d_{xz,yz}$ (90) | −11.05 | $d_{xz,yz}$ (92) | −11.11 | $d_{xz,yz}$ (81) |
| $\sigma(a_1)$ | −10.74 | $d_{z2}$ (55), Mo s (26) | −11.28 | $d_{z2}$ (54), Mo s (26) | −11.64 | $d_{z2}$ (54), Mo s (26) | −11.60 | $d_{z2}$ (36), Mo s (19) |

Least-squares fittings of $\Delta E_{1/2}$ plots vs either $\sigma_p^-$ or $\sigma_p^+$ (taken from the tabulation of Hansch *et al.*[32]) were also attempted with less satisfactory results: the correlation coefficients are 0.95 for the $\Delta E_{1/2} - \sigma_p^+$ plots of **1**, **4**, **7**, and **11** and 0.97 for the $\Delta E_{1/2} - \sigma_p^-$ plots of **1**, **4**, **7**, **8**, and **11**. This behavior parallels the early observation in the metallotetraphenylporphorins, where the influence of the phenyl substitution is best described by $\sigma$, while that of $\beta$-substitution correlates better with $\sigma_p^-$.[13] The rotational freedom of the aryl group about the $Mo_2$ coordination sphere in solution is probably responsible for the absence of a substantial delocalized contribution from the remote substituent.

The $E_{1/2}$ value for all compounds remained essentially scan rate-independent from 5 to 400 mV/s, with the largest variance determined as 18 mV. In addition, $i_p$ − (scan rate)$^{1/2}$ profiles were all linear except for **6** at high scan rate. On the basis of these observations, we believe that the values listed in Table 3 obtained under identical conditions and a scan rate of 100 mV/s represent the practical equilibrium formal reduction potentials (E°'s). Although it is apparent that the reversibility is less than ideal for most of the compounds on the basis of the difference in their anodic and cathodic peak potentials (i.e., $\Delta E_p > 60$ mV), it is not entirely evident that this is due to sluggish electron transfer rates. It is not uncommon for $\Delta E_p$− scan rate profiles to be influenced by uncompensated solution resistance in nonaqueous solvents.[33]

**Electronic Spectroscopy.** Consistent with the pale yellow color of the compounds, there is no significant absorption peak in the visible region except for a shoulder appearing in the range of 430−446 nm (2.88−2.78 eV), which is, as discussed earlier,[24] assigned as the dipole-allowed $\delta-\delta^*$ ($^1A_1 \rightarrow {}^1A_2$) transition. The narrow distribution of the $\delta-\delta^*$ transition across the series implies that the increments in both $E(\delta)$ and $E(\delta^*)$ must be approximately the same when $\sigma_X$ is increased. With the exception of compound **7**, the overall features in the UV region for all the compounds are very similar: there are one peak (around 290 nm) and three shoulders (around 380, 315, and 271 nm) which can be attributed to the LMCTs from the (−N−C−N−)-based high-energy $\pi$ orbitals to both $\delta^*$ and $\pi^*$ orbitals at the $Mo_2$ center.[24] Since the observed variance for each transition across the series (except **7**) is negligible compared with the corresponding transition energy, it is clear that the relative energy distribution of the orbitals involved in these LMCTs, i.e., $\delta^*(Mo_2)$, $\pi^*(Mo_2)$ orbitals, and nitrogen-based $\pi$ orbitals on the formamidinate ligands, is unaffected by the polar substitution. The *p*-acetyl derivative (compound **7**) is unique and has only one well-resolved absorption and one shoulder in the UV region. It is possible that there exists some hyperconjugation between the N−C−N group and the *p*-acetyl group through the phenyl ring.

**Electronic Structures.** In order to evaluate the substituent influence, all the atoms/functional groups were retained in the model calculation with one exception: replacement of the −OMe group with −OH in **1**. Although a comprehensive analysis is practically impossible since there are 160−200 occupied valence MOs, the feature of most low-energy MOs being C−C, C−H, C−N, and C−X $\sigma$ bonding and C−C and C−N $\pi$ bonding orbitals enables us to focus on those of dominant Mo contributions. Relevant information for these orbitals are summarized in Table 4. In all of the model calculations, the Mo−Mo (anti)bonding orbitals in order of the ascending energies are $\sigma(a_1)$, $\pi$(e), $\delta(b_2$, HOMO), $\delta^*(b_1$, LUMO), $\sigma^*(a_2)$, and $\pi^*$(e).[34] Thus the existence of a Mo−Mo quadruple bond ($\sigma^2\pi^4\delta^2$) in all the compounds is further confirmed on the basis of the orbital occupancy.

Fine features of the Mo−Mo (anti)bonding interactions and Mo−L bondings around the dimolybdenum core with quadruple bond are well documented,[2] and those of the model compound supported by the $[HNC(H)NH]^-$ bridge were addressed in length on the basis of Xα calculations[24] and will not be discussed here. The unique feature of the present results is that the energy levels of both Mo−Mo bonding and antibonding orbitals do depend on the substituent, and *all* of them decrease as the $\sigma_X$ increases. While the variance of energy levels is not exactly linear with $\sigma_X$, the variance of $E(\delta^*)$ is essentially the same as that of $E(\delta)$, and hence a nearly constant $\delta-\delta^*$ (HOMO−LUMO) gap (4.92, 4.84, 4.69, and 4.67 eV for **1**, **4**, **5**, and **10**, respectively) is maintained, which parallels the invariance in the observed $\lambda_{max}$-($\delta-\delta^*$) across the series. It is worth pointing out that there is no orbital contribution toward Mo−Mo bonding orbitals from the substituents, confirming the absence of the substituent contribution through delocalization. Furthermore, the Mulliken charges on the molybdenum center for **1**, **4**, **5**, and **10** are 0.505, 0.540, 0.556, and 0.571, respectively. This demonstrates that, despite the absence of direct orbital contribution to the upper valence orbitals, the electron-withdrawing substitutent does induce a buildup of positive charge on the $Mo_2$ core. On the basis of these observations we postulate that polar substitution away from the first coordination sphere is equivalent to applying a spherical electrostatic potential, which can significantly shift the absolute energy levels of the $Mo_2$ core with a minimum alternation in both the relative distribution and the composition of the upper valence molecular orbitals.

(32) Hansch, C.; Leo, A.; Taft, R. W. *Chem. Rev.* **1991**, *91*, 165.
(33) Bard, A. J.; Faulkner, L. R. *Electrochemical Methods*; Wiley: New York, 1980.

(34) The reversal of the conventional $E(\pi^*) < E(\sigma^*)$ is not unusual for the Fenske−Hall calculation of metal−metal bonded dinuclear species, and it is likely caused by the empirical approximations inherent in the Fenske−Hall method (personal communication, Dr. Xuejun Feng, Texas A&M University).

## Conclusions and Future Work

Our study demonstrates that through the remote substituent both the energy levels of frontier orbitals and the electron richness of dimolybdenum core can be significantly attenuated. The generality of this observation within the family of paddle wheel compounds is being probed with the study of formamidinate compounds of middle and late transition metals. Similar studies will be carried out with the diruthenium systems bearing both labile and less bulky bridging ligands which may catalyze reactions such as carbene-transfer, hydrogenation, and olefin metathesis.[35]

(35) (a) Lindsay, A. J.; McDermott, G.; Wilkinson, G. *Polyhedron* **1988**, *7*, 1239. (b) Noels, A. F.; Demonceau, A.; Carlier, E.; Hubert, A. J.; Marquez-Silva, R.-L.; Sanchez-Delgado, R. A. *J. Chem. Soc., Chem. Commun.* **1988**, 783. (c) Noels, A. F.; Demonceau, A.; Saive, E. *Adv. Catal. Des., Proc. Workshop 2nd.* **1992**, *2*, 73.

**Acknowledgment.** Donors of Petroleum Research Fund are thanked for partial support of this research. The NMR facility at Florida Tech is supported through an NSF grant (CHE-9013145). The authors acknowledge Dr. A. B. Brown for introducing us to ref 11b and the discussion about Hammett correlation, Dr. M. B. Hall for a copy of the Fenske−Hall program, Dr. J. Rokach and his group for various assistance, and Dr. T. R. Webb for suggesting the study of *p*-acetyl-derivatized formamidine.

**Supporting Information Available:** Tables of spetroscopic data for ligands (S1), $^{1}H$ and $^{13}C$ NMR and IR data for dimolybdenum compounds (S2), positional parameters for all atoms, anisotropic temperature factors, bond distance and angles for compounds **1**, **2**, **5** and **10** (S3−S22) and linear free energy plot $E_{1/2}$ vs $\sigma_X$ (Figure S1) (33 pages). Ordering information is given on any current masthead page.

IC960555O